HHS Public Access

Author manuscript

Explor Res Hypothesis Med. Author manuscript; available in PMC 2021 September 28.

Published in final edited form as:

Explor Res Hypothesis Med. 2021 September ; 6(3): 90–98. doi:10.14218/ERHM.2021.00011.

Evaluation of Renal Allograft Vasculature Using Non-contrast 3D Inversion Recovery Balanced Steady-state Free Precession MRA and 2D Quiescent-interval Slice-selective MRA

Ali Serhal[1,*], **Pascale Aouad**[1], **Muhamad Serhal**[2], **Ashitha Pathrose**[1], **Pamela Lombardi**[1], **James Carr**[1], **Ryan Avery**[1], **Robert R. Edelman**[1,3]

[1]Radiology, Northwestern University Feinberg School of Medicine, Chicago, IL, USA

[2]Faculty of Medical Sciences, Lebanese University, Beirut, Lebanon

[3]Radiology, Northshore University HealthSystem, Evanston, IL, USA

Abstract

Background and objectives: Renal transplant patients often require periodic imaging to evaluate the transplant vessel anastomosis for potential vascular complications. The use of non-contrast enhanced magnetic resonance angiography (NCE-MRA) techniques is encouraged in these patients because they are at increased risk of nephrogenic systemic fibrosis (NSF) due to their renal insufficiency. This study aimed to evaluate the performance of two NCE-MRA techniques (three-dimensional [3D] balanced steady-state free precession [bSSFP] with inversion recovery and quiescent-interval slice-selective [QISS]) for the evaluation of renal allograft vasculature in patients with clinical suspicion, or Doppler ultrasound, or both of arterial anastomotic stenosis.

Methods: A total of 43 patients were included in this retrospective study. Two radiologists independently scored the images from 3D bSSFP and QISS MRA sequences for image quality and confidence in anastomosis interpretation, and the degree of stenosis at the arterial anastomosis. Correlations with digital subtraction angiography (DSA) were carried out when available. In addition, inter-rater agreement was calculated.

[*]**Correspondence to**: Ali Serhal, Radiology, Northwestern University Feinberg School of Medicine, 676 N St Clair St, Chicago, IL 60611, USA. ORCID: http://orcid.org/0000-0002-3855-6915. Tel: +1-312-695-3755, Fax: +1-312-695-5645, ali.serhal@northwestern.edu.

Author contributions

Study design (AS, PA, RRE, RA), analysis and interpretation of data (AS, PA), statistical analysis (AS, PA, RRE, RA), manuscript writing, critical revision (AS, PA, MS, AP, PL, JC, RRE, RA). All authors have made a significant contribution to this study and have approved the final manuscript.

Conflict of interest

Robert R. Edelman received research support and royalties from Siemens Healthcare. The other authors report no conflicts of interest related to this publication.

Data sharing statement

Technical appendix, statistical codes, and dataset are available from the corresponding author at ali.serhal@northwestern.edu

Results: In total, 43 patients underwent QISS and 3D bSSFP MRA. For QISS, all cases were adequate for evaluation. For 3D SSFP, 86% of cases were adequate for evaluation. There was a good-to-excellent inter-rater agreement for all scores and an excellent correlation between NCE-MRA and DSA results when available (12 patients).

Conclusions: QISS and 3D SSFP showed good inter-rater agreement for image quality and stenosis grade, with more cases being of adequate image quality that used QISS. Further study is required; however, NCE-MRA shows potential as a risk-free alternative to CTA and contrast-enhanced MRA (CE-MRA) for the evaluation of arterial anastomoses in renal transplant patients.

Keywords

Renal transplant artery stenosis; Non-contrast enhanced magnetic resonance angiography; Quiescent-interval slice-selective; Angiography

Introduction

Kidney transplantation is considered to be the treatment of choice for patients with end-stage renal disease. The number of total kidney transplants performed in the USA in 2015 was 18,597,[1] with a 1-year survival rate between 80 and 95%.[2] Despite continuing improvements, postoperative complications occur in 12–20% of cases[3–5] and are due to vascular and nonvascular causes. Vascular causes occur in 3–15% of all transplants.[6] Most commonly, these include renal artery stenosis or thrombosis formation in the renal vein, with less common vascular complications that include aneurysm, pseudo-aneurysm, or arteriovenous fistula.[7] Renal artery stenosis represents 75% of all vascular complications and can leads to transplant loss.[8,9] Early detection and treatment of these complications are crucial to save the transplant and to improve morbidity and mortality.

Invasive digital subtraction angiography (DSA) remains the gold standard for vascular evaluation but is usually reserved for therapy or when the diagnosis cannot be made by noninvasive techniques. Due to its availability and noninvasiveness, color flow Doppler ultrasonography (CFDU) is the most widely performed examination for the initial evaluation of patients suspected of having post-transplant vascular complications.[5] However, this technique only estimates the degree of renal artery stenosis indirectly based on arterial flow velocity measurements, and therefore, is dependent on the visualization of the entire donor renal artery and the surgical anastomosis. Furthermore, ultrasound evaluation has often been noted to be limited by operator dependency, it is more difficult to perform and interpret in obese patients, and there is an ongoing debate on the appropriate thresholds for Doppler parameters.[10–13] Other noninvasive imaging techniques include contrast-enhanced computed tomography angiography (CTA) and contrast-enhanced magnetic resonance angiography (CE-MRA). These noninvasive angiography techniques directly measure the size of the stenotic artery or identify venous occlusions, the use of contrast agents in post-renal transplant patients has raised concerns because of studies that demonstrated the risk of nephrotoxicity due to iodine-based contrast agents in CTA and nephrogenic systemic fibrosis (NSF) due to gadolinium-based contrast agents in CE-MRA, especially if the glomerular filtration rate (GFR) is <30 mL/m/1.73 m^2.[14] Recently, several non-contrast enhanced MRA (NCE-MRA) techniques have emerged, which provide a potential alternative. At

Northwestern University, NCE-MRA is often used in post-renal transplant patients for a more detailed evaluation of vascular lesions found on CFDU or for definitive diagnosis when the CFDU is inconclusive in patients that have a strong clinical suspicion of vascular lesions. The NCE-MRA protocol (Table 1) includes two techniques that have been optimized for transplant vascular evaluation: quiescent-interval slice-selective (QISS) MRA[15] and inversion-prepared inflow-dependent three-dimensional (3D) balanced steady-state free precession (3D bSSFP) MRA.[16]

This study aimed to evaluate the image quality and diagnostic performance of NCE-MRA for the evaluation of renal transplant vasculature. The results were compared with the DSA as a reference standard when available.

Material and methods

Data collection

This HIPAA compliant retrospective study was approved by the institutional review board at Northwestern University and the requirement for written informed consent was waived. At a single academic medical center, a PACS search was performed to identify all patients that underwent NCE-MRA (QISS and 3D bSSFP) during the last 4 years for the evaluation of clinical suspicion of transplant renal artery stenosis. Clinical information that included the transplant date, GFR at the time of the exam, CFDU reports and the long-term GFR were recorded. For patients that subsequently underwent DSA for further evaluation of the allograft vasculature, angiography images were reviewed, and the exam results were collected.

Study cohort

A total of 43 patients (mean age: 56 years (range 33–76; 30 males)) were included in this study. The time from the renal transplant to the NCE-MRA date was from 10 days to 15 years (average 2.3 years). All patients were referred for clinical, or ultrasound, or both on suspicion of renal artery stenosis at the anastomosis site. In total, 41 patients (95%) underwent CFDU of the allograft vasculature at our institution before referral for MR imaging. CFDU, which was available for 41 patients, demonstrated elevated arterial velocity at the anastomosis in 34 patients (83%), a parvus tardus waveform in the arcuate arteries that was suspicious for stenosis in two patients (5%), decreased velocity and resistivity indices at the transplant artery suggested iliac stenosis in one patient (2%), and a normal CFDU but delayed graft function in four patients (10%). Two patients did not undergo a CFDU at our institution but were referred for MRA due to strong clinical suspicion (one patient) or abnormal renal scintigraphy (one patient). After the NCE-MRA examination, 12 patients (28%) underwent subsequent renal transplant angiography for further evaluation and possible treatment.

Magnetic resonance imaging

All NCE-MRA exams were performed on 1.5T scanners (MAGNETOM Avanto; Siemens Medical Solutions, Erlangen, Germany) equipped with a 12-element body phased-array coil. The imaging protocol included localizer images of the pelvis that used standard

two-dimensional (2D) bSSFP sequences in axial and coronal reformats to identify the transplanted and ipsilateral iliac vessels followed by NCE-MRA sequences (Table 1).

For 3D bSSFP MRA, the area of interest was localized by using scout images. A 150 mm-thick inversion RF pulse was applied from the top of the axial 3D slab inferiorly to suppress the signal from veins and static tissue, with an inversion time of 800–1,200 ms. The images were acquired during free-breathing without respiratory compensation and with electrocardiogram (ECG) gating. The typical scan parameters for the 3D bSSFP MRA sequence were as follows: repetition time 3.8 ms, echo time 1.9 ms; flip angle, 90°; voxel size, 1.3 × 1.3 × 2.0 mm interpolated to 0.65 × 0.65 × 1.0 mm; and field of view, 280 × 320 mm. Total scan time was approximately 3 m (1.5–3.5 m) depending on the number of acquired imaging sections and the inversion time.

The QISS MRA was acquired in an axial plane from the level of the abdominal aorta to the level of the common femoral arteries bifurcation. The QISS sequence is a 2D ECG-gated technique that relies on the application of a slice-selective saturation radiofrequency (RF) pulse to suppress the static tissue, a tracking venous saturation RF pulse to suppress venous signal, and after a quiescent-interval of approximately 230 ms, a chemical shift-selective fat saturation RF pulse and readout are applied to image the arterial inflow. Typical scan parameters for the QISS MRA sequence included: 70° flip angle, TR = 4 ms, TE = 2 ms, TI = 1,200 ms, FOV = 36 × 36 × 24 cm, and BW = ± 75 kHz with a 256 × 256 matrix for a true spatial resolution of 1.4 × 1.4 × 2 mm^3 resolution interpolated through zero-filling to 0.7 × 0.7 × 1.0 mm^3 (total scan time was approximately 5 m depending on the area covered and the heart rate).

Image analysis

The NCE-MRA images were evaluated separately by two radiologists with 5 years of experience in cardiovascular imaging. Thin multiplanar reformats and maximum intensity projection images that were derived from the 3D bSSFP and QISS MRA were used to assess image quality and stenosis grade (Fig. 1). Since the patients were referred for suspected transplant renal artery stenosis, the analysis focused on the region of anastomosis of the transplanted renal artery to the external iliac artery. For patients with an accessory transplant artery, this vessel was noted but the larger transplant artery was used for qualitative scoring. The presence of any other concomitant pathology was noted, especially arterial or venous thrombosis.

The images were rated for the image quality and the confidence in transplant arterial anastomosis interpretation, and for the degree of stenosis using a four-point Likert scale as follows: (1) overall image quality and the confidence in transplant arterial anastomosis interpretation, 0 = severe artifact or not interpretable (any type of artifact that degraded the images with no visualization of the anastomosis region or no signal in the region), 1 = moderate artifact but interpretable (presence of artifact but the anastomosis can be evaluated), 2 = good image quality, mild artifact (mild artifact in the image but the anastomosis region was only mildly affected), and 3 = excellent image quality, no artifact (perfect, homogeneous image without any type of artifact); (2) the degree of stenosis at

the anastomosis region: 0 = no stenosis, 1 = mild stenosis estimated 0–50%, 2 = moderate stenosis estimated 51–75%, and 3 = severe stenosis estimated at >75%.

Statistical analysis

Interobserver agreement for image quality and qualitative grading of stenosis between both readers and agreement in grading image quality and qualitative stenosis grading scores between the magnetic resonance imaging (MRI) sequences for each reader were analyzed using weighted kappa test (κ). Kappa interpretation was based on Altman guidelines as follows: κ<0.2, poor agreement; κ = 0.21–0.40, fair agreement; κ = 0.41–0.60, moderate agreement; κ = 0.61–0.80, good agreement; κ = 0.81–1, very good agreement. Cohen's kappa (κ) was computed using SPSS (IBM Corp. Released 2013. IBM SPSS Statistics for Windows, Version 22.0. Armonk, NY: IBM Corp).

Results

The clinical results are summarized in Table 2 and scoring for both readers are summarized in Table 3.

For overall image quality and confidence in anastomosis interpretation, all QISS images were scored as good or excellent (mild or no artifact) by reader 1 (scores 2 and 3). Reader 2 scored all images as good or excellent (scores 2 and 3) except for one study that was scored as 1 (moderate artifact). There was fair agreement (κ = 0.507, p<0.001). For 3D bSSFP MRA, reader 1 scored five studies (12%) as a severe artifact or not interpretable (score 0), two studies (4%) as a moderate artifact (score 1), and 36 studies (84%) as good or excellent (scores 2 and 3). Reader 2 scored five studies (12%) as a severe artifact or not interpretable (score 0), four studies (9%) as a moderate artifact (score 1), and 34 studies (79%) as good or excellent (scores 2 and 3). There was moderate inter-rater agreement (κ = 0.755, p<0.001).

For the degree of stenosis evaluation, for the QISS images, reader 1 rated all 43 studies for stenosis as follows: 17 studies (40%) demonstrated no evidence of stenosis, 10 studies (23%) demonstrated mild stenosis, four studies (9%) demonstrated moderate stenosis, and 12 studies (28%) demonstrated severe stenosis. Reader 2 rated all 43 studies for stenosis as follows: 18 studies (42%) demonstrated no evidence of stenosis, seven studies (16%) demonstrated mild stenosis, nine studies (21%) demonstrated moderate stenosis, and nine studies (21%) demonstrated severe stenosis. There was moderate inter-rater agreement (κ = 0.741, p<0.001).

For 3D bSSFP MRA, both readers rated 38 studies (not interpretable anastomosis in five studies for both readers) as follows: Reader 1: 17 studies (45%) demonstrated no evidence of stenosis, eight studies (21%) demonstrated mild stenosis, four studies (10%) demonstrated moderate stenosis, and nine studies (24%) demonstrated severe stenosis. Reader 2 rated 38 out of the 43 studies for stenosis as follows: 16 studies (42%) demonstrated no evidence of stenosis, nine studies (24%) demonstrated mild stenosis, five studies (13%) demonstrated moderate stenosis, and eight studies (21%) demonstrated severe stenosis. There was moderate inter-rater agreement (κ = 0.766, p<0.001).

Both techniques were compared in the evaluation of the anastomosis stenosis for both readers and there was a moderate agreement for reader 1 and a fair agreement for reader 2 (κ = 0.653 and 0.432, respectively, $p<0.001$).

Correlation with DSA: DSA was performed in 12 patients for further evaluation of the renal transplant vasculature. The results are summarized in Table 4. Out of 12 patients, 10 patients had strong imaging evidence on NCE-MRA of either post-transplant renal artery anastomosis, external iliac artery at the anastomosis, or the common iliac artery at the anastomosis site (score 2 and 3 for stenosis). One patient was referred for evaluation of a renal intra-parenchymal arteriovenous malformation that was observed on CFDU and in one patient the NCE-MRA demonstrated mild anastomotic stenosis (score 1) for both readers and underwent DSA for clinical suspicion of anastomosis significant stenosis, DSA demonstrated mild stenosis without increased pressure gradient along the stenosis and was not treated.

DSA demonstrated the presence of renal transplant artery stenosis at anastomosis in eight patients (Fig. 2), external iliac artery stenosis at the level of the renal transplant anastomosis in one patient, common iliac artery stenosis in one patient and intra-parenchymal arteriovenous fistula in one patient, not seen on NCE-MRA but seen on CFDU, this patient had normal anastomosis on both imaging modalities. One patient underwent DSA for clinical and CFDU suspicion of stenosis at the anastomosis despite only mild stenosis on QISS MRA (score 1 for both readers), subsequently, the DSA demonstrated only mild stenosis. In a patient with severe stenosis of the common iliac artery that resulted in the loss of distal intravascular signal in the transplant renal artery with 3D bSSFP, whereas the lesion was successfully visualized on QISS MRA (Fig. 3) and confirmed on DSA. Another case of severe stenosis of the external iliac artery resulted in a nondiagnostic 3D bSSFP sequence but was successfully depicted on QISS MRA and confirmed on DSA.

Discussion

NC-MRA techniques are widely used due to being risk-free, which is related to the use of gadolinium or iodine-based agents. Especially in patients with renal transplant and low GFR, clinicians tend to avoid the use of iodine contrast due to nephrotoxic effects, especially in patients with a GFR of <30. The use of a gadolinium-based agent is limited by the risk of NSF; however, this risk is low with the newer agents, but there is a newly emerging risk of the deposition of contrast in the brain that has unclear long-term significance. The QISS MRA technique is predominantly used to evaluate suspected lower extremity peripheral arterial disease.[15,17,18] To the best of our knowledge, this is the first study to investigate the use of QISS MRA in transplant renal artery assessment. QISS MRA reliably depicted post-transplant renal arterial anatomy. In addition, this study demonstrated that the combination of both NCE-MRA techniques (QISS and 3D bSSFP) could evaluate the transplant artery anastomosis for stenosis in all patients that were suspected of transplant artery stenosis with a good-to-excellent inter-rater agreement. In a small cohort of patients where DSA correlation was available, NCE-MRA accurately graded transplant anastomotic stenosis comparison with the reference standard. Both NCE techniques proved complementary: however, QISS provided diagnostic image quality in a larger proportion of the subjects,

the 3D bSSFP acquisition afforded thinner slices for improved quality of multiplanar reconstructions.

Several previous studies demonstrated that 3D bSSFP-based NCE-MRA sequences could evaluate renal transplant arteries.[8,16,19–21] In this study, adequate evaluation of transplant artery stenosis using 3D bSSFP MRA was feasible in 38 out of 43 cases (88%). Previous studies have reported slightly higher numbers, which included 87% in a study of 15 patients,[16] and 95.4% of cases in a larger study of 369 examinations.[19] The differences in the reported success rate could be related to differences in the study design, technique implementation, or patient populations.

The 3D bSSFP sequence has a scan time of few minutes, compared with approximately $\frac{1}{3}$ s for each 2D QISS slice. Consequently, the 3D bSSFP sequence had an increased risk of artifacts from respiration and bowel motion. In addition, suboptimal positioning of the in-plane inversion slab could result in saturation of the vessels of interest. Technical failure of the 3D bSSFP MRA sequence occurred in five cases in this study, further evaluation of these cases demonstrated that in two cases, the stenosis was at the common iliac and external iliac arteries proximal to the anastomosis that led to the loss of distal flow secondary to severe stenosis that was successfully depicted on the QISS images. In another three cases, there was a technical error in positioning the inversion slab that resulted in inflowing arterial blood signal suppression as the result of this error. The combination of both sequences could potentially provide more confidence in the evaluation the arterial anastomosis. In addition, one sequence could serve as a backup when the other was limited due to artifacts or technical limitations.

This study has limitations due to the small number of subjects, the retrospective nature of data acquisition, and the presence of the gold standard reference (DSA) in a small portion of subjects.

Future directions

Non-contrast MRI plays an important role in daily clinical practice. Due to the continuous development of robust non-contrast sequences, this allows for accurate imaging diagnosis, which spares the patient from the injection of contrast material. This study demonstrated the possibility of accurate arterial renal transplant evaluation using a NC-MRA technique, QISS, and confirmed the usefulness of 3D IR bSSFP MRA for this type of indication. This study is the first to report the use of the QISS sequence for this indication, to the best of the authors' knowledge, and could provide a reference for future research into the use of QISS in the evaluation of the vascular system in renal transplants for a larger cohort and the evaluation of other visceral arteries.

Conclusions

QISS and 3D SSFP showed good inter-rater agreement for image quality and stenosis grade, with more cases being of adequate image quality using QISS. In addition, there was an excellent correlation with the angiography results when DSA was performed on a subset of patients. Further study is required; however, MRA that used a combination of these NCE

techniques has potential as a risk-free alternative to CTA and CE-MRA for the evaluation of renal transplant arterial anatomy.

Funding

This study was supported by the National Institutes of Health (R01 HL130093 and R21 HL126015).

Abbreviations:

bSSFP	balanced steady-state free precession
CTA	computed tomography angiography
DSA	digital subtraction angiography
GFR	glomerular filtration rate
QISS	quiescent-interval slice-selective
NCE-MRA	non-contrast enhanced magnetic resonance angiography
NSF	nephrogenic systemic fibrosis

References

[1]. Hart A, Smith JM, Skeans MA, Gustafson SK, Stewart DE, Cherikh WS, et al.OPTN/SRTR 2015 Annual Data Report: Kidney. Am J Transplant2017;17(Suppl 1):21–116. doi:10.1111/ajt.14124. [PubMed: 28052609]

[2]. Cecka JM, Terasaki PI. The UNOS Scientific Renal Transplant Registry. Clin Transpl1992:1–16. [PubMed: 1306688]

[3]. Orons PD, Zajko AB. Angiography and interventional aspects of renal transplantation. Radiol Clin North Am1995;33(3):461–471. [PubMed: 7740106]

[4]. Shoskes DA, Hanbury D, Cranston D, Morris PJ. Urological complications in 1000 consecutive renal transplant recipients. J Urol1995;153(1):18–21. doi:10.1111/ajt.1412410.1097/00005392-199501000-00008. [PubMed: 7966766]

[5]. Brown ED, Chen MY, Wolfman NT, Ott DJ, Watson NE Jr. Complications of renal transplantation: evaluation with US and radionuclide imaging. Radiographics2000;20(3):607–622. doi:10.1148/radiographics.20.3.g00ma14607. [PubMed: 10835115]

[6]. Kobayashi K, Censullo ML, Rossman LL, Kyriakides PN, Kahan BD, Cohen AM. Interventional radiologic management of renal transplant dysfunction: indications, limitations, and technical considerations. Radiographics2007;27(4):1109–1130. doi:10.1148/rg.274065135. [PubMed: 17620470]

[7]. Reyna-Sepúlveda F, Ponce-Escobedo A, Guevara-Charles A, Escobedo-Villarreal M, Pérez-Rodríguez E, Muñoz-Maldonado G, et al.Outcomes and Surgical Complications in Kidney Transplantation. Int J Organ Transplant Med2017;8(2):78–84. [PubMed: 28828167]

[8]. Tang H, Wang Z, Wang L, Hu X, Wang Q, Li Z, et al.Depiction of transplant renal vascular anatomy and complications: unenhanced MR angiography by using spatial labeling with multiple inversion pulses. Radiology2014;271(3):879–887. doi:10.1148/radiol.14131800. [PubMed: 24592960]

[9]. Bruno S, Remuzzi G, Ruggenenti P. Transplant renal artery stenosis. J Am Soc Nephrol2004;15(1):134–141. doi:10.1097/01.asn.0000099379.61001.f8. [PubMed: 14694165]

[10]. Pan FS, Liu M, Luo J, Tian WS, Liang JY, Xu M, et al.Transplant renal artery stenosis: Evaluation with contrast-enhanced ultrasound. Eur J Radiol2017;90:42–49. doi:10.1016/j.ejrad.2017.02.031. [PubMed: 28583646]

[11]. Granata A, Clementi S, Londrino F, Romano G, Veroux M, Fiorini F, et al.Renal transplant vascular complications: the role of Doppler ultrasound. J Ultrasound2014;18(2):101–107. doi:10.1007/s40477-014-0085-6. [PubMed: 26191097]

[12]. Ngo AT, Markar SR, De Lijster MS, Duncan N, Taube D, Hamady MS. A systematic review of outcomes following percutaneous transluminal angioplasty and stenting in the treatment of transplant renal artery stenosis. Cardiovasc Intervent Radiol2015;38(6):1573–1588. doi:10.1007/s00270-015-1134-z. [PubMed: 26088719]

[13]. Fananapazir G, McGahan JP, Corwin MT, Stewart SL, Vu CT, Wright L, et al.Screening for Transplant Renal Artery Stenosis: Ultrasound-Based Stenosis Probability Stratification. AJR Am J Roentgenol2017;209(5):1064–1073. doi:10.2214/AJR.17.17913. [PubMed: 28858538]

[14]. Dekkers IA, Roos R, van der Molen AJ. Gadolinium retention after administration of contrast agents based on linear chelators and the recommendations of the European Medicines Agency. Eur Radiol2018;28(4):1579–1584. doi:10.1007/s00330-017-5065-8. [PubMed: 29063255]

[15]. Edelman RR, Sheehan JJ, Dunkle E, Schindler N, Carr J, Koktzoglou I. Quiescent-interval single-shot unenhanced magnetic resonance angiography of peripheral vascular disease: technical considerations and clinical feasibility. Magn Reson Med2010;63(4):951–958. doi:10.1002/mrm.22287. [PubMed: 20373396]

[16]. Liu X, Berg N, Sheehan J, Bi X, Weale P, Jerecic R, et al.Renal transplant: nonenhanced renal MR angiography with magnetization-prepared steady-state free precession. Radiology2009;251(2):535–542. doi:10.1148/radiol.2512081094. [PubMed: 19261926]

[17]. Edelman RR, Giri S, Dunkle E, Galizia M, Amin P, Koktzoglou I. Quiescent-inflow single-shot magnetic resonance angiography using a highly undersampled radial k-space trajectory. Magn Reson Med2013;70(6):1662–1668. doi:10.1002/mrm.24596. [PubMed: 23348595]

[18]. Serhal A, Koktzoglou I, Edelman RR. Feasibility of Image Fusion for Concurrent MRI Evaluation of Vessel Lumen and Vascular Calcifications in Peripheral Arterial Disease. AJR Am J Roentgenol2019; 212(4):914–918. doi:10.2214/AJR.18.20000. [PubMed: 30714829]

[19]. Zhang LJ, Peng J, Wen J, Schoepf UJ, Varga-Szemes A, Griffith LP, et al.Non-contrast-enhanced magnetic resonance angiography: a reliable clinical tool for evaluating transplant renal artery stenosis. Eur Radiol2018;28(10):4195–4204. doi:10.1007/s00330-018-5413-3. [PubMed: 29666993]

[20]. Bultman EM, Klaers J, Johnson KM, François CJ, Schiebler ML, Reeder SB, et al.Non-contrastenhanced 3D SSFP MRA of the renal allo graft vasculature: a comparison between radial linear combination and Cartesian inflowweighted acquisitions. Magn Reson Imaging2014;32(2):190–195. doi:10.1016/j.mri.2013.10.004. [PubMed: 24246390]

[21]. Lanzman RS, Voiculescu A, Walther C, Ringelstein A, Bi X, Schmitt P, et al.ECG-gated nonenhanced 3D steady-state free precession MR angiography in assessment of transplant renal arteries: comparison with DSA. Radiology2009;252(3):914–921. doi:10.1148/radiol.2531082260. [PubMed: 19635833]

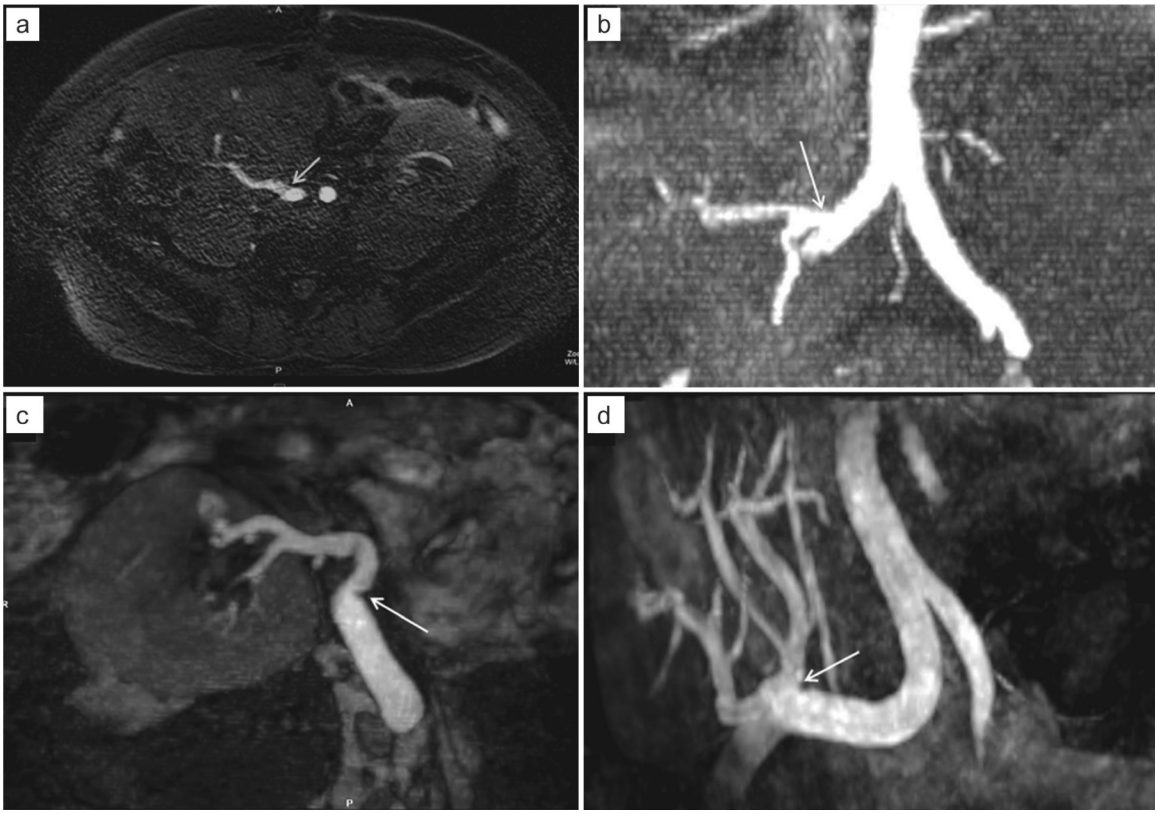

Fig. 1. Normal QISS MRA and reformat in a 48-year-old male with a 1-year history of right lower quadrant kidney transplant that presented with mild renal dysfunction (GFR = 48) and abnormal Doppler ultrasound (a and b); Normal appearance of a 3D SSFP MRA reformat in a 60-year-old female with a 3-year history of right lower quadrant kidney transplant presented with renal dysfunction (GFR = 32) and abnormal Doppler ultrasound (c and d).

No further vascular evaluation was obtained in these patients. Flow contrast improved, and motion sensitivity reduced with QISS; however, the quality of multiplanar reformats was better with 3D SSFP due to the reduced slice thickness. SSFP, steady-state free precession; QISS, quiescent-interval slice-selective; MRI, magnetic resonance imaging; SSFP, Steady-state free precession; QISS, quiescent-interval slice-selective; GFR, glomerular filtration rate; DSA, digital subtraction angiography.

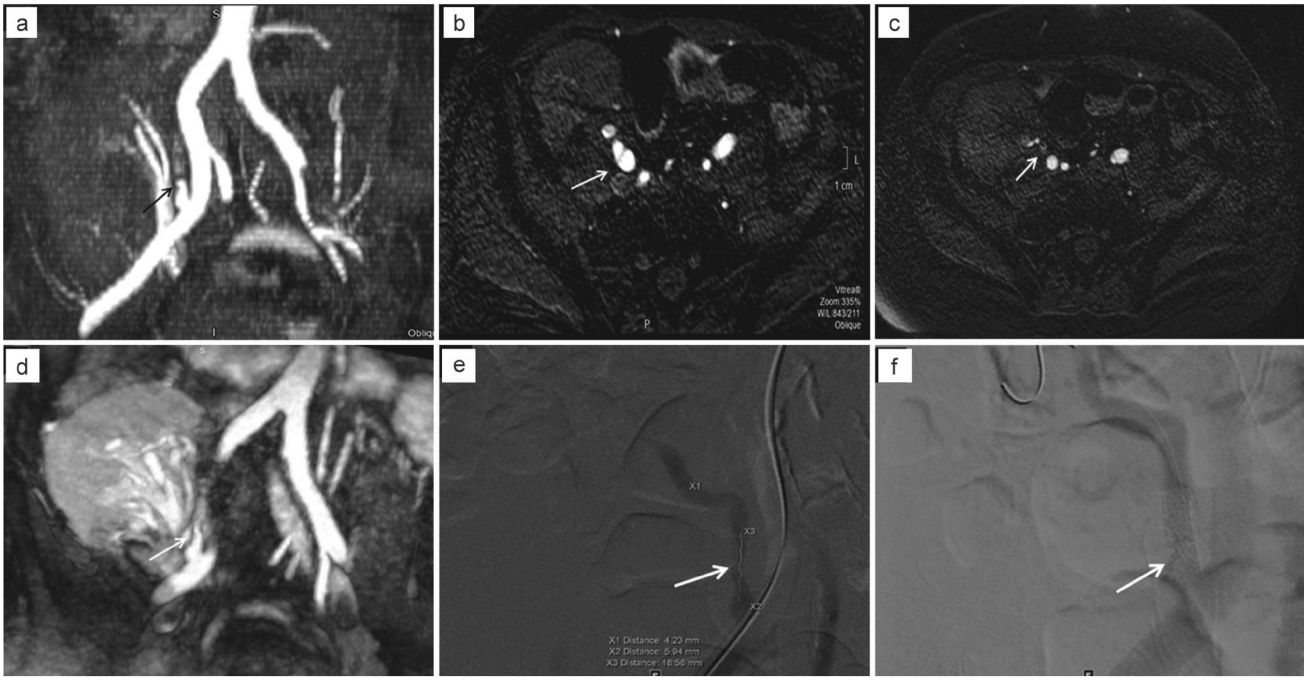

Fig. 2. 59-year-old male with right lower quadrant renal transplant presented 2 months after transplantation for evaluation high velocity at the artery anastomosis and renal dysfunction (GFR = 5).

Axial and reformats QISS MRA (a, b, and c) demonstrate obliteration of the transplant renal artery in its post anastomotic segment (arrows). The anastomosis itself is patent (arrow). 3D SSFP MRA demonstrates similar findings (arrow in (d)). The patient underwent DSA exam (e and f) that demonstrate irregularity and high-grade post anastomotic stenosis of the renal artery (arrows) treated with balloon angioplasty and stenting with improvement of the renal function post-treatment. SSFP, Steady-state free precession; QISS, quiescent-interval slice-selective; GFR, glomerular filtration rate; DSA, digital subtraction angiography.

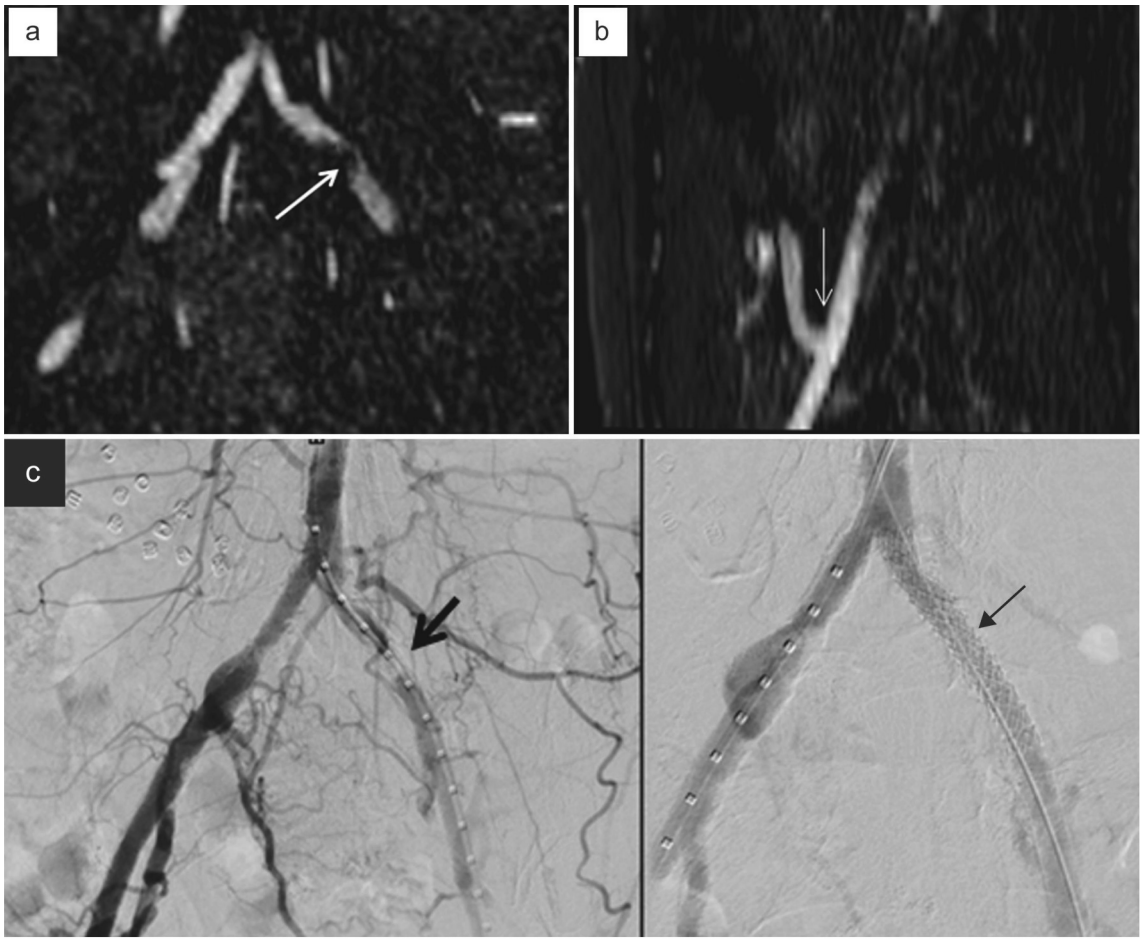

Fig. 3. 55-year-old female with left lower quadrant renal transplant in 2003 presented with transplant dysfunction (GFR = 26).

Doppler ultrasound demonstrated low velocity and resistivity index at the renal artery anastomosis concerning the proximal stenosis. Coronal reformat of QISS MRA (a) demonstrates severe stenosis of the left common iliac artery proximal to the renal transplant anastomosis (arrow). The renal anastomosis was normal on sagittal reformat of QISS MRA (b). 3D SSFP MRA was not diagnostic due to lack of signal. Patient underwent subsequent DSA (c) that showed the left common iliac stenosis (arrow) and post-stenting appearance. Of note, there was excellent correlation with the QISS MRA. The kidney function recovered post-treatment. SSFP, Steady-state free precession; QISS, quiescent-interval slice-selective; GFR, glomerular filtration rate; DSA, digital subtraction angiography.

Table 1.

Typical imaging parameters for SSFP MRA and QISS MRAs

NC-MRA sequence	SSFP MRA	QISS
Matrix	256/0/0/192	400/0/0/195
FOV (mm)	320	400
TE (ms)	1.9	1.60
TR (ms)	3.8	640.04
Section thickness (mm)	1.0	3.0
Flip angle	90	90
Bandwidth (Hz)	781	658
Excitation	Slab-selective	Slice-Selective
Mean acquisition time	3 m	5 m (approximately 0.3 s/slice)
Voxel size (mm)	1.3 × 1.3 × 2.0	0.5 × 0.5 × 3.0

MRA, Magnetic resonance imaging; SSFP, steady-state free precession; QISS, quiescent-interval slice-selective; FOV, Field of view; TE, echo time; TR, repetition time.

Table 2.

Clinical data summary of the cohort including demographics, renal function (GFR) at the time of NC-MRA imaging, peak Doppler velocity of the transplant renal artery at the anastomosis, and resistive indices of the arcuate arteries

Patient	Gender	Age (years)	Time from transplant (day)	GFR at time of MRI	Doppler velocity (cm/s)	RI at arcuate arteries
1	M	61	5,018	37	174	elevated
2	F	40	239	27	313	normal
3	F	76	10	53	216	elevated
4	M	63	36	29	308	elevated
5	M	19	98	53	440	normal
6	M	60	43	36	200	elevated
7	F	62	4,473	37	126	parvus tardus
8	F	55	5,281	26	68	low RI
9	F	65	25	27	156	elevated
10	M	60	142	32	203	elevated
11	M	63	2,334	38	294	normal
12	F	65	2,390	17	221	elevated
13	M	47	250	25	321	normal
14	F	76	113	59	487	normal
15	M	64	2,262	36	334	elevated
16	M	50	409	40	328	normal
17	F	66	197	37	436	normal
18	M	71	72	43	458	normal
19	F	19	70	45	262	normal
20	M	59	97	5	142	low RI
21	M	63	433	30	157	elevated
22	M	54	127	31	128	parvus tardus
23	M	51	47	28	236	normal
24	M	38	212	>60	347	normal
25	F	33	191	22	404	low RI
26	M	58	55	42	309	elevated
27	M	50	74	32	322	normal

Patient	Gender	Age (years)	Time from transplant (day)	GFR at time of MRI	Doppler velocity (cm/s)	RI at arcuate arteries
28	M	49	39	39	290	normal
29	M	59	3,662	36	218	normal
30	M	55	4,449	37	280	elevated
31	M	42	77	36	448	normal
32	M	46	11	35	NA	NA
33	M	71	105	32	358	normal
34	M	44	638	35	NA	NA
35	M	69	81	42	237	normal
36	M	61	454	32	203	elevated
37	F	58	5	10	372	elevated
38	M	49	480	33	412	normal
39	M	66	158	36	412	elevated
40	M	57	68	16	425	normal
41	F	68	69	27	393	normal
42	F	58	87	33	287	normal
43	M	55	309	40	318	elevated

GFR, glomerular filtration rate; RI, resistive index; MRI, magnetic resonance imaging.

Table 3.

There was good inter-rater agreement on qualitative scores for both reviewers

Overall image quality and confidence for anastomosis evaluation	Reader 1 QISS	Reader 2 QISS	Reader 1 bSSFP	Reader 2 bSSFP
0	0 (0%)	0 (0%)	5 (12%)	5 (12%)
1	0 (0%)	1 (2%)	2 (4%)	4 (9%)
2	18 (42%)	23 (54%)	18 (42%)	16 (37%)
3	25 (58%)	19 (44%)	18 (42%)	18 (42%)
Stenosis evaluation	Reader 1 QISS (N = 43)	Reader 2 QISS (N = 43)	Reader 1 bSSFP (N = 38)	Reader 2 bSSFP (N = 38)
0	17 (40%)	18 (42%)	17 (45%)	16 (42%)
1	10 (23%)	7 (16%)	8 (21%)	9 (24%)
2	4 (9%)	9 (21%)	4 (10%)	5 (13%)
3	12 (28%)	9 (21%)	9 (24%)	8 (21%)

bSSFP, Balanced steady-state free precession; QISS, quiescent-interval slice-selective.

Table 4.

Comparison between DSA and NC-MRA sequences

Patient	DSA result	QISS score reader 1	QISS score reader 2	bSSFP score reader 1	bSSFP score reader 2	Pretreatment GFR	Post-treatment GFR
2	3	3	3	3	3	27	38
4	2[a]	3	3	Not interpretable	Not interpretable	29	36
8	3[a]	3	3	Not interpretable	Not interpretable	26	>60
13[b]	0	0	0	0	0	No treatment of anastomosis	
17	3	3	3	3	2	37	>60
18	2	3	3	3	3	43	>60
20	3	3	3	3	3	5	45
28	3	3	3	3	3	39	>60
35	1	1	1	1	1	No treatment of anastomosis	
39	2	2	2	2	2	36	56
40	2	2	2	2	2	16	23
41	3	3	3	3	3	27	37

bSSFP, Balanced steady-state free precession; QISS, quiescent-interval slice-selective; GFR, glomerular filtration rate; DSA, digital subtraction angiography.

[a] stenosis is at common iliac artery or external iliac artery

[b] evaluation for renal arteriovenous malformation.